common carotid artery was significantly associated with elevated serum hs-CRP in subjects between 65 and 79 years old. However, in subjects aged 80 years or older, there was no significant relationship between max IMT and hs-CRP. Although the reason for this result is not clarified, there are possible explanations. First, our subjects aged 80 years or older were healthy community-dwelling elderly who survived up to this age without serious cardiovascular events. Second, they had relatively few risk factors compared with those in previous studies. Prevalence of diabetes and smoking were particularly low especially in those aged 80 years or older. There are several reports that have showed the direct interactions between CRP and conventional risk factors. For example, in healthy middle-aged women, who are unlikely to have cardiovascular disease, CRP had significant associations with BMI, insulin resistance and other risk factors. However, significant association between CRP and carotid artery IMT was found only in ever-smokers not in non-smokers and a risk factor such as obesity could explain a much larger part of the variance of CRP than did carotid artery IMT.[34] Although CRP has been traditionally regarded as a bystander marker of vascular inflammation, it also strongly links multiple risk factors. The priority order of these linkages has not been fully elucidated. Therefore, in our elderly objects with relatively few risk factors, association between hs-CRP and carotid IMT may be attenuated.

Cardiac events and CRP

With regard to the association between coronary artery disease and CRP, the majority of reports have targeted young and middle-aged populations. The Framingham Offspring Study investigated cytokines and vasodilatory dysfunction of the brachial artery.[35] High CRP levels and impaired coronary reserve in juvenile type I diabetes[36] and the relation between serum CRP levels and blood coagulation disorders in acute myocardial infarction aged 45 years or younger[37] were also reported. Khor et al. investigated the relation between age and the utility of CRP in 2254 patients with coronary artery disease, and reported that CRP was a useful predictor for vascular events in men and women aged less than 55 years, but not in women aged 55 years or older.[38]

To date, only a small number of studies have investigated the predictive power of inflammatory markers for cardiovascular diseases or carotid atherosclerotic lesions in the elderly aged 80 years or older. The Helsinki Aging Study[31] evaluated three elderly cohorts aged 75, 80 and 85 years to assess the predictive value of CRP for cardiovascular mortality during a 10-year follow-up. A predictive value was not found in the 80- and 85-year-old cohorts, although it was present in the 75-year-old cohort. This result was consistent with the results of our study that showed no significant relationship between

the max IMT and hs-CRP in subjects aged 80 years or older. On the other hand, the Leiden 85-plus study[32,33] showed that the subjects 85 years or older who died from stroke had significantly higher CRP level than controls, although the level of CRP in those who died from stroke was similar to that in those died from non-cardiovascular causes. Moreover, high CRP and low interleukin (IL)-10 levels had a significant relationship with history of stroke only at baseline in 85-year-old subjects. The follow-up study failed to demonstrate this relationship.

Other factors for atherosclerosis in subjects aged 80 years or older

Although aging itself may lead to increased levels of CRP and other acute phase protein,[39,40] very old subjects over 80 years were not fully investigated. In our study, although the average hs-CRP levels were comparable, the max IMT was thicker in subjects aged 80 years or older than in those less than 80 years, indicating the possible role of additional factors that may lead to the advancement of atherosclerotic lesions in the elderly.

Regarding diabetes and IMT, there have been no detailed reports in subjects aged 80 years or older. In general, IMT was significantly increased in type II diabetes patients compared with healthy subjects; a similar result was reported for juvenile type I diabetic patients with relatively few risk factors. In the elderly, diabetes is widely recognized as a risk factor for coronary heart disease, stroke and peripheral arterial disease, but it is still controversial whether the management and status of diabetes are associated with these cardiovascular diseases in those aged 80 years or older.

The Berlin Aging Study[41] demonstrated age-dependent differences in the effect of conventional risk factors in the presence of carotid plaques, although CRP was not examined in that study. The presence of carotid artery plaques had no association with either gender difference or factors related to genetic background. Total cholesterol, LDL cholesterol, total cholesterol/LDL cholesterol ratio, and BMI had significant association with carotid plaques only in those aged 70–80 years. Hypertension and diabetes had a significant association with carotid plaques only in those aged 81 years or older.

Our results were consistent with the Berlin Aging Study, because increased max IMT had a significant relation with diabetes only in subjects aged 80 years or older. Higher levels of serum Hb-A1c were also associated with thickened max IMT only in this age group although the mean value of Hb-A1c was in normal range. Further investigation is necessary to clarify the influence of relatively mild glucose intolerance on carotid atherosclerotic lesions in the elderly. In the present study, total cholesterol and LDL cholesterol had

no association with IMT in both age groups. This result may again be explained by the fact that only 14.5% of our study subjects had a history of hyperlipidemia.

Intima–media thickness and cardiovascular events

There were several large studies that used B-mode IMT measurement to identify the determinants of athero-sclerotic disease in communities such as the Rotterdam study,[12,42–44] the Atherosclerotic Risk in Communities (ARIC) study[2,45,46] and the Cardiovascular Health Study.[13] The Rotterdam study, with a cohort of 8000 subjects aged 55 years or over, has demonstrated significant associations between carotid IMT and stroke, angina and myocardial infarction. The results are consistent with that of the Cardiovascular Health Study. The ARIC study, with more than 15 000 subjects, also showed an association between thickened carotid IMT and recurrent cardiovascular disease events. Good reproducibility of carotid ultrasound was also demonstrated in this study. These large observational studies provided the evidence that IMT measurements may be a surrogate marker for atherosclerosis.

Study limitations

Although the automatic multipoint measuring software is helpful for quantitative analysis, using the data only from the common carotid artery as a representative value of atherosclerosis may be problematic and this method might have underestimated the number of carotid artery lesions. However, since the variation is large in the site of carotid artery bifurcation, evaluation including the internal carotid artery tends to yield larger variation between individuals and, therefore, we used the data of the common carotid artery

Also, we could not ascertain the types of medication and duration of treatment in subjects with hypertension, hyperlipidemia and diabetes. Use of aspirin and statin may have also influenced the level of hs-CRP although the number of subjects who underwent medical treatment were relatively small.

Small sample size and cross-sectional study design may also be limitations. A longitudinal follow-up study with a large number of subjects is necessary.

Conclusion

Our results suggest that hs-CRP and other conventional risk factors may have different significance depending on age. In particular, the predictive power of hs-CRP as a marker of atherosclerotic process was less significant in subjects aged 80 years or older.

We investigated a fairly small change of IMT in carotid arteries using automatic measuring system, which may have led to a different impact in the predic-

tive value of hs-CRP. Further longitudinal investigations on the delicate change of IMT, not cardiovascular events, will elucidate the progression of atherosclerotic lesions and related risk factors in the elderly aged over 80 years.

References

1 Berk BC, Weintraub WS, Alexander RW. Elevation of C-reactive protein in "active" coronary artery disease. *Am J Cardiol* 1990; **65**: 168–172.

2 Alexander RW. Inflammation and coronary artery disease. *N Engl J Med* 1994; **331**: 468–469.

3 Ross R. Atherosclerosis: an inflammatory disease. *N Engl J Med* 1999; **340**: 115–126.

4 Blake GJ, Ridker PM. Novel clinical marker of vascular wall inflammation. *Circ Res* 2001; **89**: 763–771.

5 Kuller LH, Tracy RP, Shaten J, Meilahn EN. Relation of C-reactive protein and coronary heart disease in the MRFIT nested case-control study. *Am J Epidemiol* 1996; **144**: 537–547.

6 Tracy RP, Lemaitre RN, Psaty BM *et al.* Relationship of C-reactive protein to risk of cardiovascular disease in the elderly. Results from the cardiovascular health study and the rural health promotion project. *Arterioscler Thromb Vasc Biol* 1997; **17**: 1121–1127.

7 Koenig W, Sund M, Frohlich M *et al.* C-reactive protein, a sensitive marker of inflammation, predicts future risk of coronary heart disease in initially healthy middle-aged men. Results from the MONICA (Monitoring Trends and Determinants in Cardiovascular Disease) Ausburg cohort study, 1984–1992. *Circulation* 1999; **99**: 237–242.

8 Ridker PM, Hennekens CH, Buring JE, Rifai N. C-reactive protein and other markers of inflammation in the prediction of cardiovascular disease in women. *N Engl J Med* 2000; **342**: 836–843.

9 Reuben DB, Cheb AI, Harris TB *et al.* Peripheral blood markers of inflammation predict mortality and functional decline in high-functioning community-dwelling older persons. *J Am Geriatr Soc* 2002; **50**: 638–644.

10 Burke GL, Evans GW, Riley WA *et al.* Arterial wall thickness is associated with prevalent cardiovascular disease in middle-aged adults. The atherosclerosis risk in communities (ARIC) study. *Stroke* 1995; **26**: 386–391.

11 Aronow WS, Ahn C, Mercando AD, Epstein S, Gutstein H, Schoenfeld MR. Association of silent myocardial ischemia with new atherothrombotic brain infarction in older patients with extracranial internal or common carotid arterial disease with and without previous atherothrombotic brain infarction. *J Am Geriatr Soc* 1995; **43**: 1272–1274.

12 Bots ML, Hoes AW, Koudstaal PJ, Hofman A, Grobbee DE. Common carotid intima-media thickness and risk of stroke and myocardial infarction: the Rotterdam study. *Circulation* 1997; **96**: 1432–1437.

13 O'Leary DH, Polak JF, Kronmal RA, Manolio TA, Burke GL, Wolfson SK Jr. The cardiovascular health study collaborative research group carotid-artery intima and media thickness as a risk factor for myocardial infarction and stroke in older adults. *N Engl J Med* 1999; **340**: 14–22.

14 Pearson TA, Mensah GA, Alexander RW *et al.* Markers of Inflammation and Cardiovascular Disease. Application to clinical and public health practice A statement for healthcare professionals from the centers for disease control and

prevention and the American Heart Association. *Circulation* 2003; 107: 499–511.

15 Wendelhag I, Liang Q, Gustavsson T, Wikstrand J. A new automated computerized analyzing system simplifies readings and reduces the variability in ultrasound measurement of intima-media thickness. *Stroke* 1997; 28: 2195–2200.

16 Dwyer JH, Sun P, Kwong-fu H, Dwyer KM, Selzer RH. Automated intima-media thickness: the Los Angeles Atherosclerosis Study. *Ultrasound Med Biol* 1998; 24: 981–987.

17 Baldassarre D, Tremoli E, Amato M, Veglia F, Bondioli A, Sirtori CR. Reproducibility validation study comparing analog and digital imaging technologies for the measurement of intima-media thickness. *Stroke* 2000; 31: 1104–1110.

18 Selzer RH, Mack WJ, Lee PL, Kwong-Fu H, Hodis HN. Improved common carotid elasticity and intima-media thickness measurements from computer analysis of sequential ultrasound frames. *Atherosclerosis* 2001; 154: 185–193.

19 Handa N, Matsumoto M, Maeda H *et al.* Ultrasonic evaluation of early carotid atherosclerosis. *Stroke* 1990; 21: 1567–1572.

20 Yamasaki Y, Kodama M, Nishizawa H *et al.* Carotid intima-media thickness in Japanese Type 2 diabetic subjects. *Diabetes Care* 2000; 23: 1310–1315.

21 Joint Committee with the Guidelines Subcommittee of the Japan Academy of Neurosonology for Ultrasonic Assessment of Carotid Artery Disease and the Subcommittee for Research into Methods of Screening Atherosclerotic Lesions. Guidelines for ultrasonic assessment of carotid artery disease: preliminary report. *Neurosonology* 2002; 15: 20–33.

22 Ridker PM, Buring JE, Rifai N. Soluble P-selectin and the risk of future cardiovascular events. *Circulation* 2001; 103: 491–495.

23 Biasucci LM, Liuzzo G, Fantuzzi G *et al.* Increasing level of interleukin (IL)-1RA and IL-6 during the first 2 days of hospitalization in unstable angina are associated with increased risk of in-hospital coronary events. *Circulation* 1999; 99: 2079–2084.

24 Ridker PM, Rifai N, Stampfer MJ, Hennekens CH. Plasma concentration of interleukin-6 and the risk of future myocardial infarction among apparently healthy men. *Circulation* 2000; 101: 1767–1772.

25 Ridker PM, Rifai N, Pfeffer M, Sacks F, Lepage S, Braunwald E. Elevation of tumor necrosis factor-α and increased risk of recurrent coronary events after myocardial infarction. *Circulation* 2000; 101: 2149–2153.

26 Ballou SP, Lozanski G. Induction of inflammatory cytokine release from cultured human monocytes by C-reactive protein. *Cytokine* 1992; 4: 361–368.

27 Bharadwaj D, Stein MP, Volzer M, Mold C, Du Clos TW. The major receptor for C-reactive protein on leukocyte s is fcgamma receptor II. *J Exp Med* 1999; 190: 585–590.

28 Pasceri V, Willerson JT, Yeh ET. Direct proinflammatory effect of C-reactive protein on human endothelial cells. *Circulation* 2000; 102: 2165–2168.

29 Hashimoto H, Kitagawa K, Hougaku H *et al.* C-reactive protein is an independent predictor of the rate of increase in early carotid atherosclerosis. *Circulation* 2001; 104: 63–67.

30 Järvisalo M, Harmoinen A, Hakanen M *et al.* Elevated serum C-reactive protein levels and early arterial changes in healthy children. *Arterioscler Thromb Vasc Biol* 2002; 22: 1323–1328.

31 Standberg TE, Tilvis RS. C-reactive protein, cardiovascular risk factors, and mortality in a prospective study in the elderly. *Arterioscler Thromb Vasc Biol* 2000; 20: 1057–1060.

32 Gussekloo J, Schaap MC, Frölich M, Blauw GJ, Westendorp RG. C-reactive protein is a strong but nonspecific risk factor of fatal stroke in elderly persons. *Arterioscler Thromb Vasc Biol* 2000; 20: 1047–1051.

33 van Exel E, Gussekloo J, de Craen AJ, Bootsma-van der Wiel A, Frolich M, Westendorp RG. Inflammation and stroke. The Leiden 85-plus study. *Stroke* 2002; 33: 1135–1138.

34 Hak AE, Stehouwer CD, Bots ML *et al.* Associations of C-reactive protein with measures of obesity, insulin resistance, and subclinical atherosclerosis in healthy, middle-aged women. *Arterioscler Thromb Vasc Biol* 1999; 19: 1986–1991.

35 Vita JA, Keaney JF Jr, Larson MG *et al.* Brachial artery vasodilator function and systemic inflammation in the Framingham offspring study. *Circulation* 2004; 110: 3604–3609.

36 Sundell J, Rönnemaa T, Laine H *et al.* High-sensitivity C-reactive protein and impaired coronary vasoreactivity in young men with uncomplicated type 1 diabetes. *Diabetologia* 2004; 47: 1888–1894.

37 Saigo M, Waters DD, Abe S *et al.* Soluble fibrin, C-reactive protein, fibrinogen, factor VII, antithrombin, proteins C and S, tissue factor, D-dimer, and prothrombin fragment 1 + 2 in men with acute myocardial infarction </=45 years of age. *Am J Cardiol* 2004; 94: 1410–1413.

38 Khor LL, Muhlestein JB, Carlquist JF *et al.* Sex- and age-related differences in the prognostic value of C-reactive protein in patients with angiographic coronary artery disease. *Am J Med* 2004; 117: 657–664.

39 Ballou SP, Lozanski FB, Hodder S *et al.* Quantitative and qualitative alterations of acute-phase proteins in healthy elderly persons. *Age Ageing* 1996; 25: 224–230.

40 Ferrucci L, Corsi A, Lauretani F *et al.* The origin of age-related proinflammatory state. *Blood* 2005; 105: 2294–2299.

41 Hillen T, Nieczaj R, Munzberg H, Schaub R, Borchelt M, Steinhagen-Thiessen E. Carotid atherosclerosis, vascular risk profile and mortality in a population-based sample of functional healthy elderly subject: the Berlin aging study. *J Intern Med* 2000; 247: 679–688.

42 Bots ML, Hofman A, Grobbee DE. Increased common carotid intima-media thickness. Adaptive response or a reflection of atherosclerosis. Findings from the Rotterdam study. *Stroke* 1997; 28: 2442–2447.

43 Iglesias del Sol A, Bots ML, Grobbee DE, Hofman A, Witteman JC. Carotid intima-media thickness at different sites: relation to incident myocardial infarction. The Rotterdam study. *Eur Heart J* 2002; 23: 934–940.

44 Hollander M, Hak AE, Koudstaal PJ *et al.* Comparison between measures of atherosclerosis and risk of stroke. The Rotterdam study. *Stroke* 2003; 34: 2367–2372.

45 Chambless LE, Heiss G, Folsom AR *et al.* Association of coronary heart disease incidence with carotid arterial wall thickness and major risk factors: the atherosclerosis risk in communities (ARIC) study, 1987–1993. *Am J Epidemiol* 1997; 146: 483–494.

46 Wattanakit K, Folsom AR, Chambless LE, Nieto FJ. Risk factors for cardiovascular event recurrence in the atherosclerosis risk in communities (ARIC) study. *Am Heart J* 2005; 149: 606–612.

ORIGINAL ARTICLE

Treatment with HMG-CoA reductase inhibitors (statins) attenuates the progression of aortic valve stenosis in the elderly

Masanori Kuwabara, Hiroaki Kitaoka, Makoto Okawa, Takashi Furuno, Masanori Nishinaga and Yoshinori Doi

Cardiology Division, Department of Medicine and Geriatrics, Kochi Medical School, Kochi, Japan

Aim: Recent studies have shown that degenerative aortic stenosis (AS) relates to the process of atherosclerosis. The purpose of this study was to determine whether the use of 3-hydroxy-3-methygulutaryl coenzyme A (HMG-CoA) reductase inhibitor (statin) delays progression of AS in the elderly.

Methods: Thirty-three elderly patients (> 65 years; mean age, 75 ± 6 years) with mild to moderate degenerative AS underwent two consecutive echocardiograms at least 6 months apart.

Results: Thirteen patients were treated with statin and the remaining 20 were not treated with statin. The two groups were similar in age (74 ± 5 vs 75 ± 6 years) and initial peak pressure gradient (45 ± 27 vs 40 ± 31 mmHg). The annual increase in peak pressure gradient in statin group was smaller than that in the non-statin group (1.25 ± 5.3 mmHg/year vs 6.04 ± 6.12 mmHg/year, $P < 0.05$). In multiple regression analysis, statin usage was an independent predictor of a smaller increase in peak gradient after adjusting for age, initial peak gradient, diabetes mellitus and hypertension.

Conclusions: Statin-treated patients had delayed AS progression compared with those not treated with statin. In the elderly, statin treatment may delay the rate of progression of degenerative AS.

Keywords: aortic valve stenosis, elderly, statin.

Introduction

Non-rheumatic, degenerative aortic valve stenosis (AS) with trileaflet valves is common in elderly people, with a prevalence of 2 to 7% in the population above 65 years of age.[1,2] Due to recent increases in the elderly population and decrease in the occurrence of rheumatic fever, the clinical significance of degenerative AS in elderly

people has been increasing.[1,2] This disease has been thought to be a consequence of degeneration of the aortic valve due to aging. However, recent studies have suggested that degenerative AS may be related to the atherosclerotic process, including deposition of lipids, macrophage infiltration and production of osteopontin, rather than simply aging.[3–7] In addition, the progression of degenerative AS has been correlated with atherosclerotic risk factors such as hypertension, smoking, and higher levels of lipoprotein (a) and low density lipoprotein.[8–12]

The purpose of this study was to determine whether the use of 3-hydroxy-3-methygulutaryl coenzyme A (HMG-CoA) reductase inhibitor (statin) delays the progression of AS in the elderly.

doi: 10.1111/j.1447-0594.2006.00331.x

Methods

Study patients

Among 12 353 patients who underwent examinations in our echocardiographic laboratory between 1 January 1994 and 31 December 2002, we retrospectively reviewed data obtained from patients who were more than 65 years old and who had undergone two consecutive echocardiograms at least 6 months apart. Patients with a calcified aortic valve and peak aortic transvalvular flow velocity of > 2 m/s as determined by transthoracic echocardiography (TTE)[13] at initial evaluation were included. Echocardiography was performed using standard practice guidelines[14] and commercially available ultrasound instruments. Peak pressure gradients across the aortic valve were calculated by the modified Bernoulli equation using continuous-wave Doppler recordings from the highest velocity available from apical views. Patients with rheumatic heart disease, a known bicuspid aortic valve, left ventricular systolic dysfunction (% fractional shortening <25%), a history of valvular surgery, other significant valvular disease, congenital heart disease, familial and combined hyperlipidemia and end-stage renal disease requiring dialysis were excluded.

Finally, thirty-three patients, 13 males and 20 females, met our study criteria. The mean age of the patients was 75 ± 6 years. Mean initial velocity was 3.1 ± 1.0 m/s and mean initial peak pressure gradient was 41.9 ± 29.4 mmHg. The patients were divided into two groups: a group of patients who were treated with statin (statin group, n = 13) and a group of patients who were not treated with statin (non-statin group, n = 20). Use of statin was determined from patient charts. Initiation of treatment with a lipid-lowering agent was performed at the discretion of the patient's primary physician. The agents used, numbers of patients, and daily doses were as follows: pravastatin, eight patients, 10 mg; simvastatin, three patients, 10 mg; atrovastatin, two patients, 10 mg.

Degree of AS progression

Annual rate of change in peak velocity was calculated by:[15]

(peak velocity at follow up − peak velocity at initial evaluation) × 12/peak velocity at initial evaluation × interval (months)

In the same way, annual rate of change in peak pressure gradient was calculated by:

(peak pressure gradient [PG] at follow up − peak PG at initial evaluation) × 12/peak PG at initial evaluation × interval (months)

Statistical analysis

Data are presented as means ± SD. Statistical analysis was carried out using a commercially available statistical package (Statview Ver.4.0, SAS Institute, Cary, NC, USA). Comparisons between the two groups were made by analysis of unpaired t-tests. A P-value <0.05 was considered statistically significant.

Results

Basic characteristics

Basic characteristics of the subjects are shown in Table 1. The statin group and the non-statin group were similar in age, prevalence of diabetes mellitus, hypertension and angiotensin-converting enzyme (ACE) inhibitor or angiotensin-receptor blocker (ARB) usage. At the initial evaluation, total cholesterol level in the statin group was over 220 mg/dL. However, the two groups showed similar total cholesterol levels at the second evaluation.

Serial change in degree of AS

As shown in Table 1, there was no significant difference between the two groups in systolic blood pressure, % fractional shortening, peak velocities and peak pressure gradients at the initial evaluation. However, the annual increase in peak velocity in the statin group (0.01 ± 0.21 m/s) was significantly smaller than that in the non-statin group (0.22 ± 0.24 m/s) (P = 0.014) (Fig. 1), and the annual increase in peak pressure gradient in the statin group (1.3 ± 5.3 mmHg) was significantly smaller than that in the non-statin group (6.0 ± 6.1 mmHg) (P = 0.028) (Fig. 2). There was also no significant correlation between the interval of echocardiograms and the annual increase in peak pressure gradients (r = −0.06, P = 0.75).

In simple and multiple regression analysis, statin usage was an independent predictor of a smaller increase in peak gradient after adjusting for age, initial peak gradient, diabetes mellitus, hypertension and ACE inhibitor or ARB usage (Table 2).

Discussion

Our study indicates that statin therapy may inhibit the progression of calcified AS in elderly patients with AS, as demonstrated by smaller increases in peak aortic velocity and pressure gradient in the treated patients.

Impact of statin on progression of AS

Rapid progression of AS was observed in patients with some atherosclerotic risk factors, including hypertension, hyperlipidemia with elevated low-density lipoprotein (LDL)-cholesterol and lipoprotein (a) levels, and

Table 1 Basic characteristics between statin group and no statin group

	Statin (n = 13)	No statin (n = 20)	P-value
Age	74 ±5	75 ±5	n.s.
Male gender, n (%)	5 (38%)	8 (40%)	n.s.
Initial systolic blood pressure (mmHg)	139 ±12	137 ±27	n.s.
Initial percentage fractional shortening (%)	40 ±8.4	37 ±5.6	n.s.
Initial PV (m)	3.20 ±0.99	3.02 ±1.01	n.s.
Initial peak PG (mmHg)	44.5 ±27.4	40.3 ±31.1	n.s.
Interval (months)	31 ±23	30 ±20	n.s.
Total cholesterol (mg/dL) at initial evaluation	214 ±35	163 ±29	0.015
Total cholesterol (mg/dL) at second evaluation	188 ±46	169 ±38	n.s.
Hypertension, n (%)	12 (92%)	14 (70%)	n.s.
Diabetes mellitus, n (%)	6 (46%)	3 (15%)	n.s.
ACE inhibitor or ARB usage, n (%)	4 (31%)	4 (20%)	n.s.

PG, pressure gradient; PV, peak velocity; ACE, angiotensin-converting enzyme; ARB, angiotensin-receptor blocker.
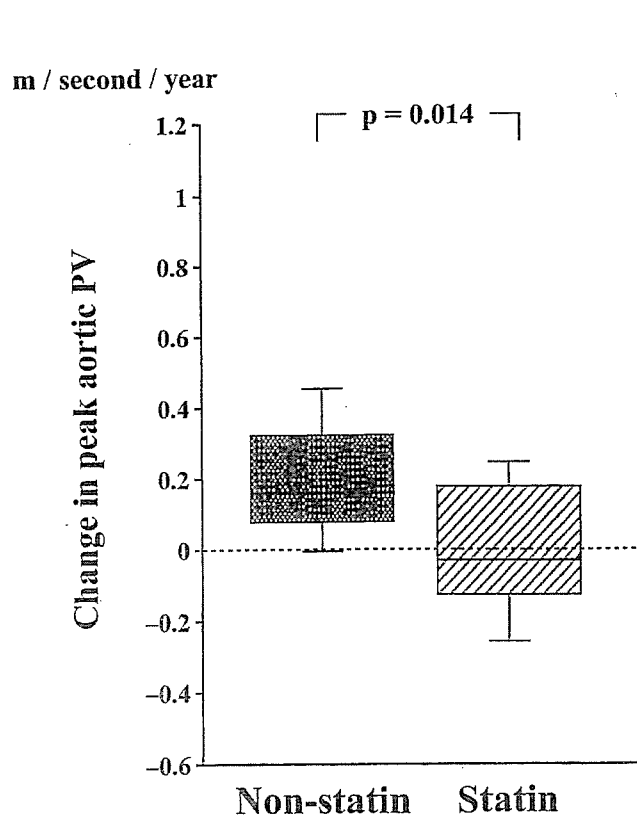

Figure 1 Annual rate of change in peak aortic velocity. The annual increase in peak velocity (PV) in the statin group was significantly smaller than that in the non-statin group.
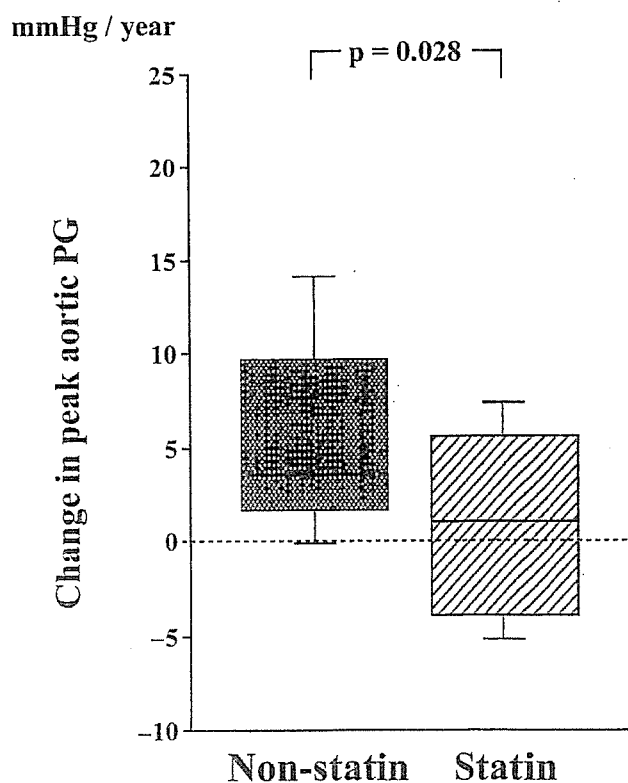

Figure 2 Annual rate of change in peak aortic pressure gradient (PG). The annual increase in peak pressure gradient in the statin group was significantly smaller than that in the non-statin group.

Table 2 Simple and multiple regression analysis

	Coefficient (simple)	P	Coefficient (multiple)	P
Age at initial evaluation	0.23	n.s.	0.18	n.s.
Pressure gradient	0.25	n.s.	0.33	n.s.
Statin usage	−0.38	<0.05	−0.48	<0.05
Diabetes mellitus	−0.17	n.s.	0.13	n.s.
Hypertension	0.05	n.s.	0.16	n.s.
ACE inhibitor or ARB usage	−0.09	n.s.	−0.01	n.s.

smoking.[8,11,16,17] In addition, calcification of degenerative AS of trileaflet valves has shown that these degenerative changes simulate those of atherosclerotic plaque.[3-6]

Therefore, it is reasonable to hypothesize that statin may be protective in the progression of calcified AS by modifying atherosclerotic process.[15,18] Shavelle *et al.* serially evaluated aortic valve calcium using electron-beam computed tomography (EBT) and found a lower rate of calcium accumulation in patients who were treated with statin.[15] Novaro *et al.* followed 174 patients (mean age, 68 ± 12 years) with mild to moderate AS (initial peak aortic gradient: 21–38 mmHg) and found smaller increases in peak and mean gradients and a smaller decrease in aortic valve area in patients who were treated with statin during a mean follow-up period of 21 months.[18] Our study patients were much older compared to these previous studies, but the results are consistent with those of the previous studies. Symptomatic severe AS is associated with a poor prognosis and often requires aortic valve replacement, with relatively high mortality and morbidity in old people.[19] Therefore, medical therapy that reduces the progression of the disease will have a great clinical significance.

Inhibitory effect of statin on AS progression

Although the mechanism by which statin therapy slow the progression of AS is unclear, it is likely that the lipid-lowering effect of statin contributes to the reduction of AS progression. A relationship between change in LDL-cholesterol level and change in valve gradient in AS patients treated with statin was previously reported. It suggests that oxidized LDL cholesterol plays a role in the pathogenesis and progression of calcified AS.[18] Also, a strong influence of LDL cholesterol level on the progression of aortic valve calcification and coronary calcification was shown when evaluated by EBT.[12]

In our study population, total cholesterol levels after treatment in the statin-treated patients were not significantly different from that in those not treated with statin, suggesting some additive effects of statin therapy beyond lipid-lowering. Statin therapy reduces monocyte adhesiveness and plaque calcification.[20,21] Early

lesions of calcified aortic valve disease appear to involve an active inflammatory process, including deposition of lipids (apo B, apo [a] and apo [E]) and infiltration of macrophages and T-cells by osteopontin and tenascin-C.[3-6,22] Therefore, the anti-inflammatory effects of statin may play a role in attenuation of the progression of calcified AS.

Study limitation

There are some limitations in this study. First, this was a retrospective study with a small study population. Second, we did not measure aortic valve area and assessed the severity of stenosis only by aortic jet velocity and peak pressure gradient, which are flow-dependent. However, because we excluded patients with left ventricular systolic dysfunction or moderate to severe aortic regurgitation either in the initial or follow-up echocardiograms, we believe that the increases in peak aortic jet velocity and pressure gradient reflect the true change of AS severity. Finally, because of the retrospective nature of the study, we could not evaluate precise lipid profiles or other biochemical factors such as C-reactive protein. A recently reported randomized trial suggested that statin therapy could not halt the progression of calcific AS. However, the report was small in sample size (77 patients in statin and 78 in placebo) and with short follow up (25 months). Further large-scale, long-term, randomized controlled studies are required in order to clarify whether statin therapy for patients with degenerative AS delays the disease progression and thereby hopefully prevents the need for valve replacement in elderly people.[23]

References

1 Lindroos M, Kupari M, Heikkila J, Tilvis R. Prevalence of aortic valve abnormalities in the elderly: an echocardiographic study of a random population sample. *J Am Coll Cardiol* 1993; 21: 1220–1225.
2 Pomerance A, Darby AJ, Hodkinson HM. Valvular calcification in the elderly: possible pathogenic factor. *J Gerontol* 1998; 33: 672–675.
3 Otto CM, Kuusisto J, Reichenbach DD, Gown AM, O'Brien KD. Characterization of the early lesion of

"degenerative" valvular aortic stenosis: histological and immunohistochemical studies. *Circulation* 1994; 90: 844–853.

4 O'Brien KD, Reichenbach DD, Macrovina SM, Kusistro L, Alpers CE, Otto CM. Apolipoprotein B and E accumulate in the morphologically early lesion of degenerative valvular aortic stenosis. *Arterioscler Thromb Vasc Biol* 1996; 16: 523–532.

5 O'Brien KD, Kusistro J, Reichenbach DD *et al.* Osteopontin is expressed in human aortic valvular lesions. *Circulation* 1995; 92: 2163–2168.

6 Olsson M, Dalsgaard C-J, Haegerstrand A, Rosenqvist M, Ryden L, Nilsson J. Accumulation of T lymphocytes and expression of interleukin-2 recepters in nonrheumatic stenotic aortic valves. *J Am Coll Cardiol* 1994; 23: 1162–1170.

7 Kitaoka H, Okawa M, Kuwabara M *et al.* Comparison of thoracic aortic atherosclerotic plaque by echocardiography in patients with stenotic tricuspid versus bicuspid aortic valves. *Am J Cardiol* 2003; 91: 895–896.

8 Gotoh T, Kuroda T, Yamasawa M *et al.* Correlation between lipoprotein (a) and aortic valve sclerosis assessed by echocardiography (the JMS Cardio Echo and Cohort Study). *Am J Caldiol* 1995; 76: 928–932.

9 Aronow WS, Schwarts KS, Koenigsberg M. Correlation of serum lipids, calcium, and phosphorus, diabetes mellitus and history of systemic hypertension with presence or absence of calcified or thickened aortic cusps or root in elderly patients. *Am J Cardiol* 1987; 59: 998–999.

10 Lindroos M, Kupari M, Valvanne J, Strandgerg T, Heiklia J, Tilvis R. Factors associated with calcific aortic valve degeneration in the elderly. *Eur Heart J* 1994; 15: 965–970.

11 Stewart BF, Siscovick D, Lind BK *et al.* Clinical factors associated with calcific aortic valve disease. *J Am Coll Cardiol* 1997; 29: 630–634.

12 Pohle K, Popers D, Moshage W, Stilianakis N, Daniel WG, Achenbach S. Progression of aortic calcification: association with coronary atherosclerosis and cardiovascular risk factors. *Circulation* 2001; 104: 2205–2209.

13 Faggiano P, Antonini-Canterin F, Erlicher A *et al.* Progression of aortic valve sclerosis to aortic stenosis. *Am J Cardiol* 2003; 91: 99–101.

14 Schiller NB, Shah PM, Crawford M *et al.* Recommendations for quantitation of the left ventricle by 2- dimensional echocardiography. *J Am Soc Echocardiogr* 1989; 2: 358–367.

15 Shavelle DM, Takasu J, Budoff MJ, Mao SS, Qiao X, O'Brien KD. HMG CoA reductase inhibitor (statin) and aortic valve disease. *Lancet* 2002; 359: 1125–1126.

16 Palta S, Pai AM, Gill KS, Pai RA. New insights into the progression of aortic stenosis implications for secondary prevention. *Circulation* 2000; 101: 2497–2502.

17 Wilmshurst PT, Stevenson RN, Griffiths H, Lord JR. A case-control investigation of the relation between hyperlipidemia and calcific aortic valve stenosis. *Heart* 1997; 78: 475–479.

18 Novaro GM, Tiong IY, Pearce GL, Lauer MS, Sprecher DL, Griffin BP. Effect of hydroxymethyl-glutaryl coenzyme A reductase inhibitors on the progression of calcific aortic stenosis. *Circulation* 2001; 104: 2205–2209.

19 Logeais Y, Langanay T, Roussin R *et al.* Surgery for aortic stenosis in elderly patients. A study of surgical risk and predictive factors. *Circulation* 1994; 90: 2891–2898.

20 Weber C, Erl W, Weber KS, Weber PC. HMG-CoA reductase Inhibitors decrease CDIIb expression and CDIIb-dependent adhesion of monocytes to endothelium and reduce increased adhesiveness of monocytes isolated from patients with hypercholesterolemia. *J Am Coll Cardiol* 1997; 30: 1212–1217.

21 Williams JK, Sukhova GK, Herrington DM, Libby P. Pravastatin has cholesterol-lowering independent effects on the artery wall of atherosclerotic monkeys. *J Am Coll Cardiol* 1998; 31: 684–691.

22 Satta J, Melkko J, Pollanen R *et al.* Progression of human aortic valve stenosis is associated with tenascin-C expression. *J Am Coll Cardiol* 2002; 39: 96–101.

23 Cowell SJ, Newby DE, Prescott RJ *et al.* A randomized trial of intensive lipid-lowering therapy in calcific aortic stenosis. *N Engl J Med* 2005; 352: 2389–2397.

ELSEVIER

Signaling pathway of nitric oxide production induced by ginsenoside Rb1 in human aortic endothelial cells: A possible involvement of androgen receptor

Jing Yu [a], Masato Eto [b], Masahiro Akishita [b], Akiyo Kaneko [a], Yasuyoshi Ouchi [b], Tetsuro Okabe [a,*]

[a] Department of Integrated Traditional Medicine, University of Tokyo Graduate School of Medicine, Tokyo, Japan
[b] Department of Gerontology, University of Tokyo Graduate School of Medicine, Tokyo, Japan

Abstract

Ginsenosides have been shown to stimulate nitric oxide (NO) production in aortic endothelial cells. However, the signaling pathways involved have not been well studied in human aortic endothelial cells. The present study was designed to examine whether purified ginsenoside Rb1, a major active component of ginseng could actually induce NO production and to clarify the signaling pathway in human aortic endothelial cells. NO production was rapidly increased by Rb1. The rapid increase in NO production was abrogated by treatment with nitric oxide synthetase inhibitor, L-NAME. Rb1 stimulated rapid phosphorylation of Akt (Ser473), ERK1/2 (Thr202/Thr204) and eNOS (Ser1177). Rapid phosphorylation of eNOS (Ser1177) was prevented by SH-5, an Akt inhibitor or wortmannin, PI3-kinase inhibitor and partially attenuated by PD98059, an upstream inhibitor for ERK1/2. Interestingly, NO production and eNOS phosphorylation at Ser1177 by Rb1 were abolished by androgen receptor antagonist, nilutamide. The results suggest that PI3kinase/Akt and MEK/ERK pathways and androgen receptor are involved in the regulation of acute eNOS activation by Rb1 in human aortic endothelial cells.
© 2006 Elsevier Inc. All rights reserved.

Keywords: Ginsenoside Rb1; Endothelial cells; Nitric oxide; eNOS; Androgen receptor; PI3-kinase; Akt; ERK; MEK; Phosphorylation

Ginseng, the root of Panax ginseng C.A. Meyer (Araliaceae), is a well-known and popular herbal medicine used worldwide. Among more than 30 ginsenosides, the active ingredient of ginseng, ginsenoside Rb1 is regarded as the main compound responsible for many pharmaceutical actions of ginseng. The oral administration of ginseng caused a decrease in blood pressure in essential hypertension [1]. Intravenous administration of ginsenosides (a mixture of saponin from Panax ginseng C.A. Meyer) lowered blood pressure in a dose-dependent manner in anesthetized rats [2]. Although these reports suggest that ginsenosides could stimulate the production of nitric oxide (NO) by aortic vascular endothelial cells, the precise mechanisms of the

ginsenoside actions have not been fully elucidated [3]. NO released from endothelial cells via the endothelial nitric oxide synthetase (eNOS) is a pivotal vasoprotective molecule. In addition to its vasodilating feature, endothelial NO has anti-atherosclerotic properties, such as inhibition of platelet aggregation, leukocyte adhesion, smooth muscle cell proliferation, and expression of genes involved in atherosclerosis [4].

The present study aims at investigating the signaling pathways involved in NO production by purified ginsenoside Rb1 in human aortic endothelial cells in vitro.

Materials and methods

Materials. Rb1, nilutamide, L-NAME (hydrochloride), Hanks' balanced salt solution (HBSS) were purchased from Sigma (St. Louis, MO,

---

* Corresponding author. Fax: +813 5684 3987.
  E-mail address: okabe-tky@umin.ac.jp (T. Okabe).

USA). ICI182780 was from Zeneca Pharmaceuticals (Macdesfield, UK). 4,5-diaminofluorescin diacetate (DAF-2 DA) was purchased from Daiichi (Daiichi Pure Chemicals Co., Ltd, Tokyo, Japan). PD98059, SH-5, wortmannin and Nitric Oxide Synthase Assay Kit were from Calbiochem (EDM Biosciences, Inc., La Jolla, CA, USA and Germany). L-[^{3}H]Arginine was purchased from Amersham (Amersham Biosciences, Uppsala, Sweden). Antibody of phospho-eNOS (Ser1177) was from upstate (Upstate Inc., Lake Placid, NY). Antibody for eNOS/NOS type III was purchased form BD Transduction Laboratories (BD Biosciences, Franklin Lakes, NJ, USA). All other antibodies were form Cell Signaling Technology (Beverly, MA, USA). LumiGLO Reserve Chemiluminescent Substrate Kit was from KPL (Gaithersburg, MD, USA). EBM-2 (endothelial cell base medium) was from Clonetics (Walkersville, MD, USA). Human aortic endothelial cells (HAECs) were from Cambrex (Cambrex BioScience Walkersville, Inc. Walkersville, MD, USA). Fetal bovine serum (FBS) was from CCT (Sanko Junyaku Co., Ltd, Tokyo, Japan), Fetal bovine serum charcoal stripped was from MultiSer (ThermoTrace Ltd., Melbourne, Australia).

Cell culture. HAECs were cultured in a 37 °C humidified atmosphere of 95% air/5% CO_2 in EGM-2 (endothelial cell grows medium 2) medium supplemented with 10% FBS. The EGM-2 medium consisted of 0.1% EGF, 0.04% hydrocortisone, 0.4% hFGF-B, 0.1% VEGF, 0.1% R^3-IGF-1, 0.1% ascorbic acid, 0.1% GA-1000, and 0.1% heparin. Experiments were performed with cells from passages 5 to 7. For all experiments, HAECs were plated at a concentration of 1×10^4/mL and grown to confluence. Then cells were serum-starved for 6 h in phenol red free EBM-2 containing 1% DCC-FBS, that was removed the steroid by processing it with dextran-coated charcoal (DCC-FBS). In some inhibitory experiments, the inhibitors were added to cells 60 min before the stimuli. DMSO was used as a solvent for Rb1, PD98059, wortmannin, SH-5, L-NAME, nilutamide, and DAF-2 DA present at equal concentrations (0.01%) in all groups, including the vehicle.

Western blot analysis. After treatment with reagents, confluent monolayers of cells were washed two times in ice-cold phosphate-buffered saline and lysed with buffer containing 20 mmol/L Tris–HCl (pH 7.5), 150 mmol/L NaCl, 1 mmol/L EDTA, 1 mmol/L EGTA, 1% Triton-X, 2.5 mmol/L sodium pyrophosphate, 1 mmol/L β-glycerophosphate, 1 mmol/LNa$_3$VO$_4$, 1 µg/mL Leupeptin, 1 mM PMSF). For western blot analysis, total cell lysate was subjected to SDS–polyacrylamide gel electrophoresis (PAGE), and proteins were transferred to poly vinilidene difluoride (PVDF) membrane. The antibodies used in this study were anti-phospho-ERK1/2 (Thr202/Thr204), anti-ERK1/2, anti phospho-Akt (Ser473), anti-Akt, anti-phosph-eNOS (ser1177) and anti-NOS. Antibodies were detected by means of a horseradish peroxidase-linked secondary antibody and immunoreactive bands were visualized using LumiGLO Reserve Chemiluminescent Substrate Kit.

Endothelial NO synthase activity assay. Endothelial cell NO synthase (eNOS) activity was quantified by measuring the conversion of L-[^{3}H]-arginine to L-[^{3}H]-citrulline by the use of a NO synthase assay kit.

Measurement of intracellular production of NO. Production of NO was assessed using the NO-sensitive fluorescent dye DAF-2 DA [5]. Briefly, confluent cells were serum-staved for 6 h. Because NOS generates O_2^- instead of NO in the absence of L-arginine, so L-arginine (100 µmol/L) was add 1 h prior to all solutions, except for the experiment with *N*-nitro-L-arginine methyl ester (L-NAME; a NOS inhibitor)-treated cells. Cells were loaded with DAF-2 DA (final concentration 5 µmol/L, 30 min 37 °C) and than rinsed three times with HBSS, kept in the dark, and maintained at 37 °C in 1% EBM-2 medium with a warming stage. After 30 min, cells were then treated with Rb1 or other stimuli. In some inhibitory experiments, the inhibitors were administered 30 min before loading with DAF-2 DA. Green fluorescence intensity was measured with a laser scanning confocal microscopy system (LSCM) (Bio-Rad Laser Sharp2000). The fluorescence image was obtained as a 512 × 512 pixel frame. Ex = 488 nm, EM = 510 nm. All other settings, including scanning speed, pinhole diameter, and voltage gain, remained the same for all experiments.

Statistics. Data are means ± SEM. Statistical comparisons were performed by Student's *T* test between two groups. A value of *P* < 0.05 was considered significant.

Results

Rb1 stimulates rapid production of NO in human aortic endothelia cells

We used the NO-specific fluorescent dye DAF-2 DA to evaluate the effect of Rb1 on NO production in HAECs. 5, 10, 15, 30, 60, 120 and 180 min after Rb1 treatment, cells were fixed and then viewed using a fluorescence microscope. Emission of green light (510 nm) from cells excited by light at 488 nm is indicative of NO production. A significant increase in green fluorescence was observed >15 min after the addition of Rb1 and lasted for 60 min in HAECs (Fig. 1A). Maximal stimulation of NO production was obtained at 30 min.

To verify that the rapid increase in green fluorescence in response to Rb1 treatment specifically reflected NO production, we compared results from HAECs treated with acetylcholine (1 µmol/L) or Rb1 (1 µmol/L) for 5 min. Reassuringly, treatment with either acetylcholine and calcium ionophore or Rb1 resulted in a increase in green fluorescence (Fig. 1B). We next examined the effects of the NOS inhibitor L-NAME to determine whether the NO increase was attributable to NOS derived de novo synthesis. As shown in Fig. 1C, the Rb1-induced DAF-2 DA fluorescence was completely suppressed by pretreatment with L-NAME (0.5 mmol/L). The results suggested that the rapid increase in NO production after Rb1 treatment was mediated by an increase in NOS activity.

Rb1 stimulates phosphorylation of eNOS (Ser1177) and increases NOS activity

To examine involvement of eNOS in the NO increase, the effect of Rb1 on eNOS phosphorylation at Ser-1177 was tested by Western blotting. As shown in Fig. 2, Rb1 induced rapid eNOS phosphorylation after 10 min of incubation, maximal eNOS phosphorylation by Rb1 was observed from 30 to 60 min of incubation. The relative magnitude of eNOS phosphorylation falls subsequently but is still significantly greater than control after 120 min of Rb1 incubation (Fig. 2A, upper blots). The acute effect by Rb1 on eNOS phosphorylation was concentration dependent (Fig. 2B, upper blots). Rb1 did not affect eNOS protein expression (Fig. 2A and B, lower blots).

To see whether Rb1 actually activates NOS in HAECs, we measured NOS activity after 30 min of treatment with Rb1. As shown in Fig. 2C, Rb1 significantly increased NOS activity in HAECs.

PI3-kinase/Akt and MEK/ERK pathways are involved in eNOS phosphorylation and NO production

Previous studies have demonstrated that PI3-kinase/ Akt and MEK/ERK pathways are two important signaling cascades mediating eNOS activation by many stimuli in vascular endothelial cells [6,7]. Therefore, we examined
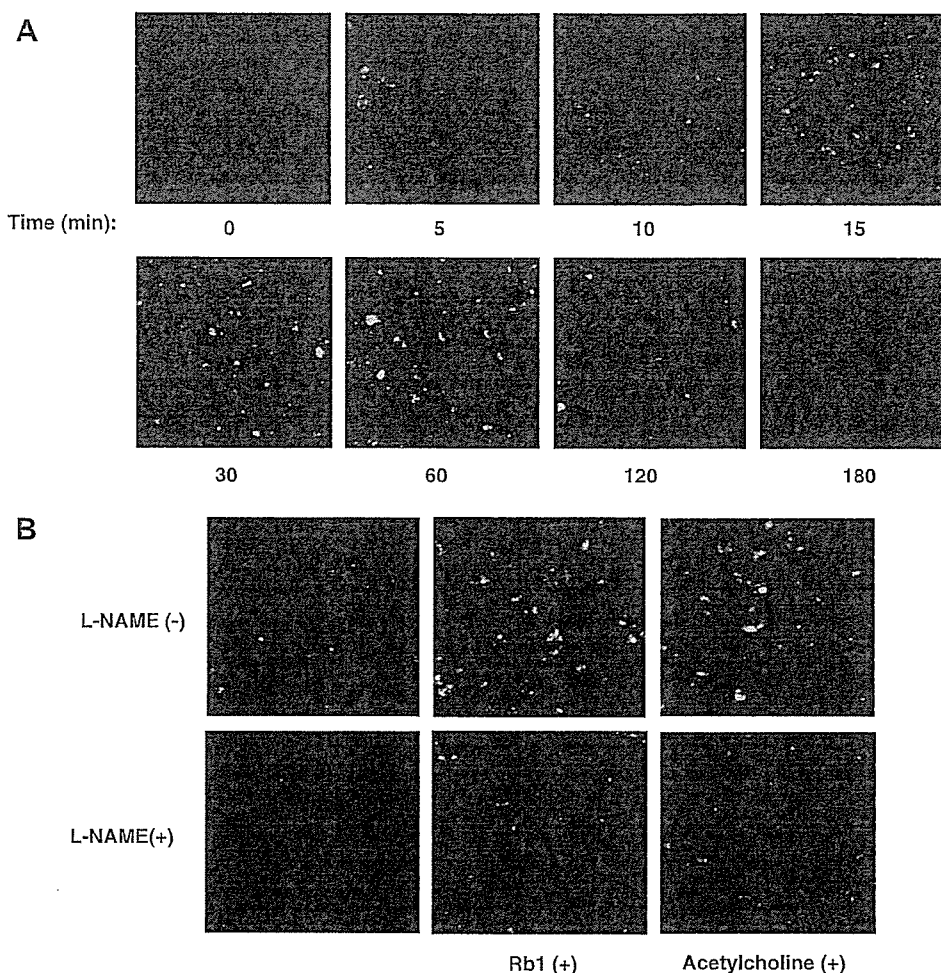
A

Time (min): 0   5   10   15

30   60   120   180

B

L-NAME (-)

L-NAME(+)

Rb1 (+)   Acetylcholine (+)

Fig. 1. Effect of Rb1 on production of NO. HAECs were starved and loaded with DAF-2 DA (5 μmol/L) as described in Materials and methods prior to treatment with either Rb1 (1 μmol/L) for 0, 5, 10, 15, 30, 60, 120, and 180 min (A) or acetylcholine (1 μmol/L) for 5 min (B). After Rb1 treatment, cells were fixed in 2% paraformaldehyde for 10 min at 4 °C and then viewed using a fluorescent microscope. Emission of green light (510 nm) from cells excited by light at 488 nm is indicative of NO production. In some groups of cells, L-NAME (0.5 mmol/L) was added 30 min before loading cells with DAF-2 DA (B). A representative time course experiment is shown for experiments that were repeated independently for three times. (For interpretation of the references to color in this figure legend, the reader is referred to the web version of this paper.)

A

p-eNOS(ser^{1177})

total NOS

Rb1 (1 μmol/L)   0   5   10   15   30   60   12   (min)

B

p-eNOS(ser^{1177})

total NOS

Rb1 (μmol/L)   -   0.01   0.1   1   10

C

$p<0.01$

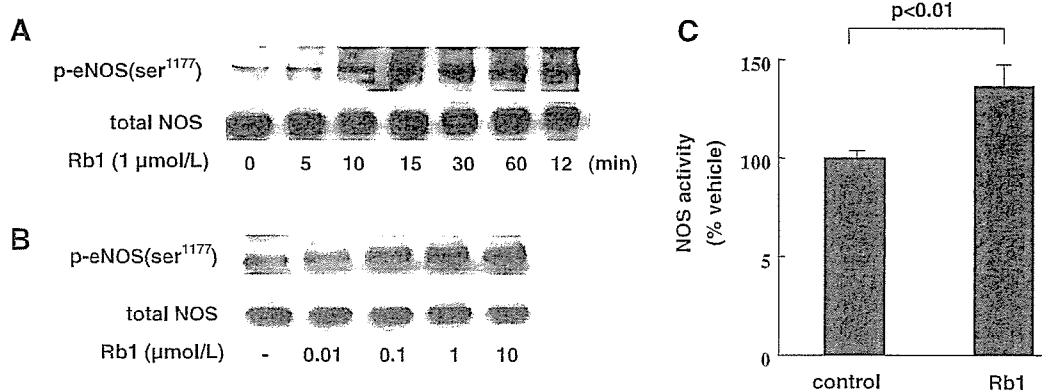NOS activity (% vehicle)

control   Rb1

Fig. 2. Effects of Rb1 on eNOS phosphorylation and NOS activity. Phosphorylation of eNOS in HAECs. Starved HAECs were treated with the vehicle (0.01% DMSO) or Rb1 (1 μmol/L) for indicated times (A) or with various concentrations of Rb1 for 30 min (B). Western analysis performed to detect phospho-eNOS (Ser1177) and total eNOS. The experiments were repeated three times in triplicates, with equal result. NOS activity in HAECs homogenates. Rb1 (1 μmol/L) were added to the starved medium for 30 min, then activity of NOS was measured by the conversion of L-arginine to L-citrulline at 37 °C for 60 min (C). Histograms and error bars represent means ± SEM of four independent experiments performed in duplicate. *P < 0.01 vs control.

whether Rb1 activated Akt and ERK1/2. We used phospho-specific antibodies to evaluate the ability of Rb1 to stimulate phosphorylation of Akt and ERK1/2 in HAECs. Rb1 rapidly increased phosphorylation of Akt (Ser473) and ERK1/2 (Fig. 3A, upper blots) in HAECs > 5 min after the addition of Rb1. Maximal phosphorylation was attained at 30 min in Akt and at 15 min in ERK1/2. The relative magnitude of the Rb1 response falls subsequently but is still significantly greater than control after 120 min of Rb1 treatment. Rb1 did not affect total Akt and ERK protein expression (Fig. 3A, lower blots).

We next examined the rapid phosphorylation of eNOS at Ser1179 by Rb1 either in the absence or presence of PI3 kinase inhibitor wortmannin, and Akt inhibitor SH-5 or MEK (ERK kinase) inhibitor PD98059. As shown in Fig. 3B, the rapid eNOS phosphorylation was abolished by pretreatment of cells with wortmannin (5 μmol/L) or SH-5, and partially attenuated by MEK inhibitor PD98059 (10 μmol/L). NO production viewed by fluorescent microscopy showed the similar inhibition by these inhibitors (Fig. 3C). These results suggest that acute activation of eNOS and NO production by Rb1 were mediated through activation of PI3-kinase/Akt and ERK1/2.
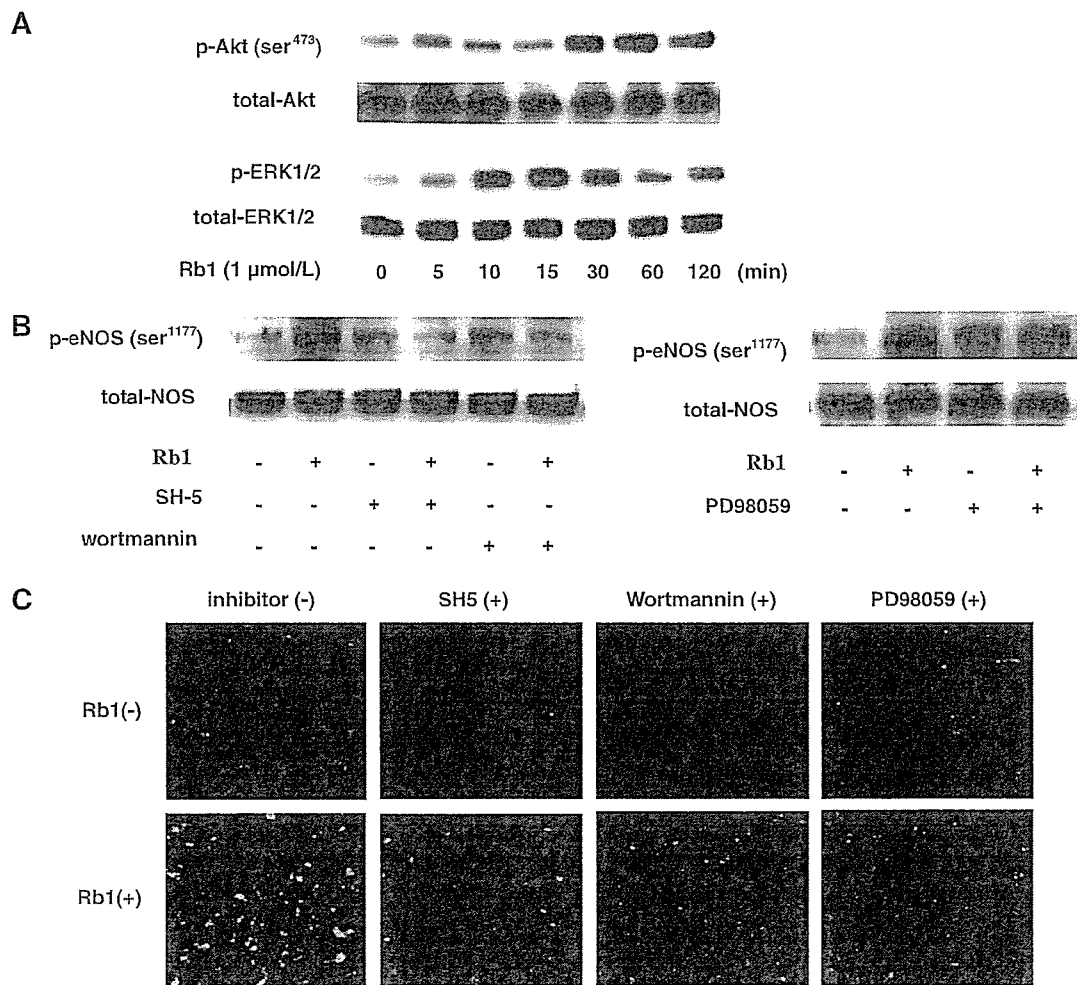

Fig. 3. Effects of inhibitors for PI3kinae/Akt or MEK (ERK kinase) on eNOS phosphorylation and NO production. Starved HAECs were treated with the vehicle (0.01% DMSO) or Rb1 (1 μmol/L) for indicated times (A). In some groups, cells were pretreated with SH-5 (10 μmol/L), wortmannin (5 μmol/L) or PD98059 (10 μmol/L) for 1 h, then cells were treated without or with Rb1 (1 μmol/L) for 30 min (B). Cell lysates were analyzed by Western blot as described in Materials and methods. Anti-phospho-Akt (Ser473) antibody and anti-Akt antibody; anti-phospho-ERK1/2 antibody and anti-ERK1/2 antibody (A), anti-phospho-eNOS (Ser1177) antibody and anti-eNOS antibody (B) were used for western blot analysis. Experiments were repeated three times, with equivalent result. Starved cells were loaded with DAF-2 DA as described in Materials and methods before treatment with Rb1 (1 μmol/L). In some groups of cells, SH-5 (10 μmol/L), wortmannin (5 μmol/L) or PD98059 (10 μmol/L) were added 60 min before cells were loaded with DAF-2 DA. After Rb1 treatment, cells were fixed in 2% paraformaldehyde for 10 min at 4 °C and then viewed using a fluorescent microscope (C). Emission of green light (510 nm) from cells excited by light at 488 nm is indicative of NO production. A representative set of experiments is shown for experiments that were repeated independently three times. (For interpretation of the references to color in this figure legend, the reader is referred to the web version of this paper.)
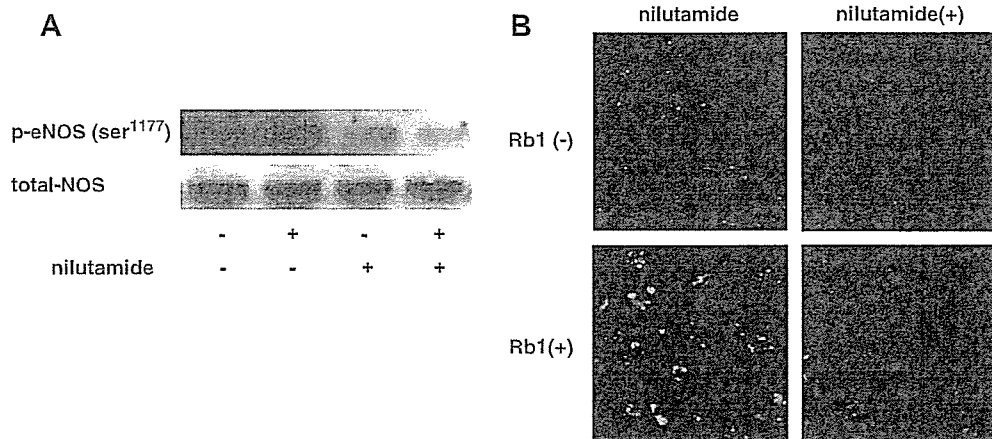
Fig. 4. Effects of nilutamide, an antagonist of androgen receptor, on eNOS phosphorylation and NO production. HAECs were starved 6 h and then treated without or with Rb1 (1 μmol/L) for 30 min. Some groups of cells were pre-treated with androgen receptor agonist nilutamide (10 μmol/L) for 1 h. Cell lysates were then subjected to immunoblotting as described in Materials and methods. The experiments were repeated three times in triplicates, with equal results. Starved cells were loaded with DAF-2 DA as described in Materials and methods before treatment with Rb1 (1 μmol/L). In some groups of cells, nilutamide (10 μmol/L) were added 60 min before cells were loaded with DAF-2 DA. After Rb1 treatment, cells were fixed in 2% paraformaldehyde for 10 min at 4 °C and then viewed using a fluorescent microscope (B). Emission of green light (510 nm) from cells excited by light at 488 nm is indicative of NO production. The experiments were repeated independently three times with equal results. (For interpretation of the references to color in this figure legend, the reader is referred to the web version of this paper.)

Rb1-induced eNOS phosphorylation is inhibited by androgen receptor antagonist

Increasing evidence shows that activation of the steroid hormone receptor such as estrogen receptor (ER) lead to NO production and vasodilation within minutes by non-transcriptional pathways. Ginsenosides have steroidal skeleton structure and can act as an agonist for steroid hormones receptor. To see whether steroid hormone receptors were involved in acute activation of eNOS to produce NO in HUACs by Rb1, we examined the effects of the androgen receptor antagonist nilutamide and estrogen receptor antagonist ICI182780. Representative western blots obtained using anti-phospho-eNOS (Ser1177) antibody and anti-eNOS antibody are shown in Fig. 4A. The Rb1-induced eNOS phosphorylation (Ser1177) was inhibited by the androgen receptor antagonist nilutamid (10 μmol/L) In addition, NO production was diminished to the baseline level in the presence of nilutamid (Fig. 4B). However, the Rb1-induced eNOS phosphorylation (Ser1177) and NO production were unaffected by an estrogen receptor (ER) antagonist ICI182780 (10 μmol/L) (data not shown).

Discussion

We have shown that purified Rb1 rapidly stimulates production of NO in HAECs > 15 min after treatment. Maximal stimulation of NO production was obtained at 30 min. The increase in NO production was abrogated by the addition of eNOS inhibitor, L-NAME. It is generally well known that eNOS is tightly regulated not only at the transcriptional level but also by several post-transcriptional

mechanisms [8]. The enhanced phosphorylation at Ser1177 leads to increased eNOS activity. In our experiments, Rb1 induced rapid phosphorylation of eNOS at Ser1177 > 10 min after Rb1 treatment. Maximal eNOS phosphorylation by Rb1 was observed from 30 to 60 min of incubation. NOS activity was also increased by the addition of Rb1 in HAECs. Taken together, our results suggest that the acute effect on NO production in HAECs is attributable to rapid phosphorylation of eNOS at Ser1177. NO produced by eNOS is a fundamental determinant of cardiovascular homeostasis responsible for regulating systolic blood pressure, vascular remodeling and angiogenesis. It is possible to consider that Rb1, a major active component of ginseng could be a candidate responsible for the antihypertensive effects of ginseng previously reported [1,2].

Recent studies have revealed that PI3-kinase/Akt and MEK/ERK1/2 pathways are crucial regulator in cell proliferation, cell-cycle progression, and mediator of cellular survival. Both of them also contribute to enhanced phosphorylation of eNOS at Ser1177/1179 and production of NO [6,7]. The present study showed that Rb1 also stimulated the phosphorylation of Akt (Ser473) and ERK1/2 (Thr202/Thr204) in HAECs. Rb1-induced eNOS phosphorylation was prevented by inhibitors for PI3-kinase/Akt or MEK (ERK kinase). Our data suggest that the activation of PI3-kinase/Akt and MEK/ERK-mediated pathways are involved in the regulation of acute eNOS phosphorylation by ginsenoside Rb1 in HAECs.

Another interesting finding is that acute phosphorylation of eNOS by Rb1 was abolished by an antagonist for androgen receptor. Recent studies have shown Rb1 acts as a phytoestrogen in MCF-7 human mammary carcinoma

cells [9]. However, in HAECs, Rb1-induced eNOS phosphorylation was not prevented by an antagonist for estrogen receptor (data not shown). It is known that testosterone prevents coronary artery disease, and lower testosterone level is a risk factor for ischemic heart disease in men [10–12]. Recent studies revealed that endothelial NO has antiatherosclerotic properties, such as inhibition of platelet aggregation, leukocyte adhesion, smooth muscle cell proliferation, and expression of genes involved in atherosclerosis [4]. Together with these observations, our results that Rb1 induced eNOS phosphorylation has been abolished by the androgen receptor antagonist will be the beginning of the experimental analyses at cellular levels and may provide a clue for better understanding of the mechanisms by which androgens exert their action for preventing coronary artery disease. Further studies are required for elucidation.

Acknowledgments

References

[1] K.H. Han, S.C. Choe, H.S. Kim, D.W. Sohn, K.Y. Nam, B.H. Oh, M.M. Lee, Y.B. Park, Y.S. Choi, J.D. Seo, Y.W. Lee, Effect of red ginseng on blood pressure in patients with essential hypertension and white coat hypertension, Am. J. Chin. Med. 26 (1998) 199–209.

[2] N.D. Kim, S.Y. Kang, V.B. Schini, Ginsenosides evoke endothelium-dependant vascular relaxation in rat aorta, Gen. Pharmacol. 25 (1994) 1071–1077.

[3] N.D. Kim, S.Y. Kang, J.H. Park, V.B. Schini-Kerth, Ginsenoside Rg3 mediates endothelium-dependent relaxation in response to ginsenosides in rat aorta: role of K^+ channels, Eur. J. Pharmacol. 367 (1999) 41–49.

[4] A.G. Herman, S. Moncada, Therapeutic potential of nitric oxide donors in the prevention and treatment of atherosclerosis, Eur. Heart J. 26 (2005) 1945–1955.

[5] H. Kojima, N. Nakatsubo, K. Kikuchi, S. Kawahara, Y. Kirino, H. Nagoshi, Y. Hirata, T. Nagano, Detection and imaging of nitric oxide with novel fluorescent indicators: diaminofluoresceins, Anal. Chem. 70 (1998) 2446–2453.

[6] X. Peng, S. Haldar, S. Deshpande, K. Irani, D.A. Kass, Wall stiffness suppresses Akt/eNOS and cytoprotection in pulse-perfused endothelium, Hypertension 41 (2003) 378–381.

[7] D. Feliers, X. Chen, N. Akis, G.G. Choudhury, M. Madaio, B.S. Kasinath, VEGF regulation of endothelial nitric oxide synthase in glomerular endothelial cells, Kidney Int. 68 (2005) 1648–1659.

[8] I. Fleming, R. Busse, Molecular mechanisms involved in the regulation of the endothelial nitric oxide synthase, Am. J. Physiol. Regul. Integr. Comp. Physiol. 284 (2003) R1–R12.

[9] J. Cho, W. Park, S. Lee, W. Ahn, Y. Lee, Ginsenoside-Rb1 from Panax ginseng C.A. Meyer activates estrogen receptor-alpha and -beta, independent of ligand binding, J. Clin. Endocrinol. Metab. 89 (2004) 3510–3515.

[10] G.B. Phillips, B.H. Pinkernell, T.Y. Jing, The association of hypotesteronemia with coronary artery disease in men, Arterioscler. Thromb. 14 (1994) 701–706.

[11] C.M. Webb, J.G. McNeill, C.S. Hayward, D. De Zeigler, P. Collins, Effects of testosterone on coronary vasomotor regulation in men with coronary heart disease, Circulation 100 (1999) 1690–1696.

[12] F.C. Wu, A. von Eckardstein, Androgens and coronary artery disease, Endocr. Rev. 24 (2003) 183–217.

ELSEVIER

Gas6/Axl-PI3K/Akt pathway plays a central role in the effect of statins on inorganic phosphate-induced calcification of vascular smooth muscle cells

Bo-Kyung Son [a], Koichi Kozaki [b], Katsuya Iijima [a], Masato Eto [a], Toru Nakano [c], Masahiro Akishita [a], Yasuyoshi Ouchi [a,*]

[a] *Department of Geriatric Medicine, Graduate School of Medicine, The University of Tokyo, 7-3-1 Hongo, Bunkyo-ku, Tokyo 113-8655, Japan*
[b] *Department of Geriatric Medicine, Kyorin University School of Medicine, Tokyo, Japan*
[c] *Discovery Research Laboratory, Shionogi and Co., Ltd., Osaka, Japan*

Abstract

Apoptosis is essential for the initiation and progression of vascular calcification. Recently, we showed that 3-hydroxy-3-methylglutaryl (HMG) CoA reductase inhibitors (statins) have a protective effect against vascular smooth muscle cell calcification by inhibiting apoptosis, where growth arrest-specific gene 6 (Gas6) plays a pivotal role. In the present study, we clarified the downstream targets of Gas6-mediated survival signaling in inorganic phosphate (Pi)-induced apoptosis and examined the effect of statins. We found that fluvastatin and pravastatin significantly inhibited Pi-induced apoptosis and calcification in a concentration-dependent manner in human aortic smooth muscle cells (HASMC), as was found with atorvastatin previously. Gas6 and its receptor, Axl, expression were downregulated in the presence of Pi, and recombinant human Gas6 (rhGas6) significantly inhibited apoptosis and calcification in a concentration-dependent manner. During apoptosis, Pi suppressed Akt phosphorylation, which was reversed by rhGas6. Wortmannin, a specific *phosphatidylinositol 3-OH kinase* (PI3K) inhibitor, abolished the increase in Akt phosphorylation by rhGas6 and eliminated the inhibitory effect of rhGas6 on both Pi-induced apoptosis and calcification, suggesting that PI3K-Akt is a downstream signal of the Gas6-mediated survival pathway. Pi reduced phosphorylation of Bcl2 and Bad, and activated caspase 3, all of which were reversed by rhGas6. The inhibitory effect of statins on Pi-induced apoptosis was accompanied by restoration of the Gas6-mediated survival signal pathway: upregulation of Gas6 and Axl expression, increased phosphorylation of Akt and Bcl2, and inhibition of Bad and caspase 3 activation. These findings indicate that the Gas6-mediated survival pathway is the target of statins' effect to prevent vascular calcification.
© 2006 Elsevier B.V. All rights reserved.

Keywords: Calcification; Apoptosis; Gas6; Axl; Akt; Bcl2

1. Introduction

Vascular calcification, such as coronary and aortic calcification, is clinically important in the development of cardiovascular disease (Eggen, 1968). Two distinct forms of vascular calcification are well recognized. One is medial calcification, which occurs between the cell layers of smooth muscle cells and is related to aging, diabetes and chronic renal failure (Neubauer, 1971; Goodman et al., 2000). The other is atherosclerotic calcification, which occurs in the intima during the development of

atheromatous disease (Wexler et al., 1996). In diabetic patients, medial calcification has been shown to be a strong independent predictor of cardiovascular mortality (Everhart et al., 1988).

We recently demonstrated that atorvastatin prevented inorganic phosphate (Pi)-induced calcification by inhibiting apoptosis, one of the important processes regulating calcification. This was mediated by growth arrest-specific gene 6 (Gas6), a vitamin K-dependent protein (Son et al., 2006). Gas6 binds to Axl, the predominant receptor for Gas6, on the cell surface and transduces the signal by Axl autophosphorylation (Mark et al., 1996). Gas6-Axl interaction has been shown to be implicated in the regulation of multiple cellular functions (Yanagita et al., 2001; Goruppi et al., 1996; Nakano et al., 1997; Fridell et al., 1998). Especially, they are known to protect a range of cell types

from apoptotic death (Goruppi et al., 1996, 1999; Healy et al., 2001). However, the downstream targets of Gas6-mediated signaling in Pi-induced apoptosis and the effect of statins on this pathway are poorly understood.

With respect to the targets of Gas6-Axl interaction, Lee et al. (2002) showed that activation of Akt is necessary for Gas6-dependent cell survival. Akt is an important mediator of metabolic and survival responses after growth factor stimulation. Akt is activated by phosphorylation, which is performed by phosphatidylinositol 3-OH kinase (PI3K), a kinase that is activated by Gas6-Axl interaction (Lee et al., 2002; Ming Cao et al., 2001). Activation of Akt leads to downstream signaling events including those associated with mitochondrial regulators of apoptosis such as Bcl2 and Bad.

In the present study, we examined the effect of statins using two different types: lipophilic fluvastatin and hydrophilic pravastatin. We investigated the effect of statins on Pi-induced apoptosis and calcification as well as on signaling components in this process. Consequently, we found that both statins restored the Gas6-mediated survival pathway, with upregulation of the expression of Gas6 and Axl, increased phosphorylation of Akt, Bcl2 and Bad; and finally inhibition of caspase 3 activation, resulting in the prevention of apoptosis and subsequent calcification in human aortic smooth muscle cells (HASMC).

2. Materials and methods

2.1. Materials

Pravastatin and fluvastatin were supplied by Sankyo Co. Ltd. and Tanabe Seiyaku Co., Ltd., respectively. Recombinant human Gas6 (rhGas6) was prepared as described previously (Ming et al., 2001). Wortmannin was purchased from Calbiochem. All other reagents were of analytical grade.

2.2. Cell culture

HASMC were obtained from Clonetics. They were cultured in Dulbecco's modified Eagle's medium (DMEM) supplemented with 20% *fetal bovine serum* (FBS), 100 U/ml penicillin and 100 mg/ml streptomycin at 37 °C in a humidified atmosphere with 5% CO_2. HASMC were used up to passage 8 for the experiments.

2.3. Induction and quantification of calcification

For Pi-induced calcification, Pi (a mixed solution of Na_2HPO_4 and NaH_2PO_4 whose pH was adjusted to 7.4) was added to serum-supplemented DMEM to a final concentration of 2.6 mM. After the indicated incubation period, cells were decalcified with 0.6 M HCl, and Ca content in the supernatant was determined by the o-cresolphthalein complexone method (C-Test, WAKO). The remaining cells were solubilized in 0.1 M NaOH/0.1% *sodium dodecyl sulfate* (SDS), and cell protein content was measured by Bio-Rad protein assay. Calcification was visualized by von Kossa's method. Briefly, the cells were

fixed with 4% formaldehyde and exposed to 5% aqueous $AgNO_3$.

2.4. Induction and determination of apoptosis

Two different time courses were tested to investigate Pi-induced apoptosis and examine the effect of statins, under short-term (within 24 h) and long-term (up to 10 days) conditions (Son et al., 2006).

2.4.1. TdT-mediated dUTP nick end-labeling (TUNEL) assay

TUNEL assay to detect DNA fragmentation was performed using a commercially available kit (ApopTag Plus, Chemicon). Briefly, the samples were preincubated with equilibration buffer for 10 min, and subsequently incubated with terminal deoxyribonucleotidyl transferase in the presence of digoxigenin-conjugated dUTP for 1 h at 37 °C. The reaction was terminated by incubating the samples in stopping buffer for 30 min. After 3 rinses with *phosphate-buffered saline* (PBS), a fluorescein-labeled anti-digoxigenin antibody was applied for 30 min, and the samples were rinsed 4 times with PBS. The samples were then stained, mounted with DAPI (*4',6-diamino-2-phenylindole*)/antifade, and examined by fluorescence microscopy.

2.4.2. Detection of DNA fragmentation by ELISA

Cytoplasmic histone-associated DNA fragments were determined with a cell-death detection ELISA^{plus} kit (Roche) as a quantitative index of apoptosis. Briefly, after the cells were incubated in lysis buffer for 30 min, 20 μl of the cell lysates was used for the assay. Following addition of substrate, colorimetric change was determined as the absorbance value measured at 405 nm.

2.5. Immunoblotting

The effect of Pi and statins on the expression of Gas6 and Axl, phosphorylation of Akt, Bcl2 and Bad, and activation of caspase 3 was examined at 12 h. The collected cell lysates were applied to SDS-polyacrylamide gels under reducing conditions, and transferred to a polyvinylidene difluoride (PVDF) membrane. Immunoblot analysis was performed using specific primary antibodies: anti-Axl, anti-Gas6 (Santa Cruz Biotechnology), anti-caspase 3, anti-Akt, anti-Bcl2, anti-phospho-Akt, anti-phospho-Bcl2, anti-phospho-Bad (Cell Signaling Technology), and anti-Bad (Transduction Laboratories). After incubation with horseradish peroxidase-conjugated secondary antibodies (Amersham Pharmacia), blots were visualized by enhanced chemiluminescence and autoradiography (ECL Plus, Amersham Pharmacia). Experiments were performed with at least three different cell populations.

2.6. Statistical analysis

All results are presented as mean±S.E.M. Statistical comparisons were made by ANOVA, unless otherwise stated. A value of $P < 0.05$ was considered to be significant.

3. Results

3.1. Statins inhibit Pi-induced apoptosis and calcification in HASMC

In HASMC, a high Pi level (≥ 2.6 mM), comparable to that of hyperphosphatemia in end-stage renal disease, significantly induced calcification. Fluvastatin showed an inhibitory effect on Pi-induced calcification at as high a concentration as 0.1 μM (26.1±2.3% of control), while pravastatin showed the degree of effect at 50 μM (27.4±3.1% of control) (Fig. 1A). An inhibitory effect on Ca deposition was also found by von Kossa's staining (Fig. 1B). Both statins prevented Pi-induced apoptosis at the same concentrations as those at which they prevented calcification (Fig. 1C). An antiapoptotic effect of statins was also observed by TUNEL assay on day 6 (Fig. 1D).

3.2. Gas6 plays an important role in Pi-induced apoptosis

In the presence of 2.6 mM Pi, the expression of Gas6 and Axl was markedly downregulated (Fig. 2A). To investigate the role of Gas6 in Pi-induced apoptosis and calcification, first, we tested whether supplementation of rhGas6 could prevent Pi-induced apoptosis. In HASMC, rhGas6 significantly inhibited Pi-induced apoptosis in a concentration-dependent manner (Fig. 2B). Furthermore, during apoptosis, activated products of caspase 3 (17 and 19 kDa) were significantly increased by 2.6 mM Pi, which was reversed by rhGas6 (Fig. 2C). Next, we examined the effect of rhGas6 on calcification. Recombinant human Gas6 significantly inhibited Pi-induced calcification on day 6 in a concentration-dependent manner (Fig. 2D), suggesting that Gas6 plays an important role in Pi-induced apoptosis and calcification.
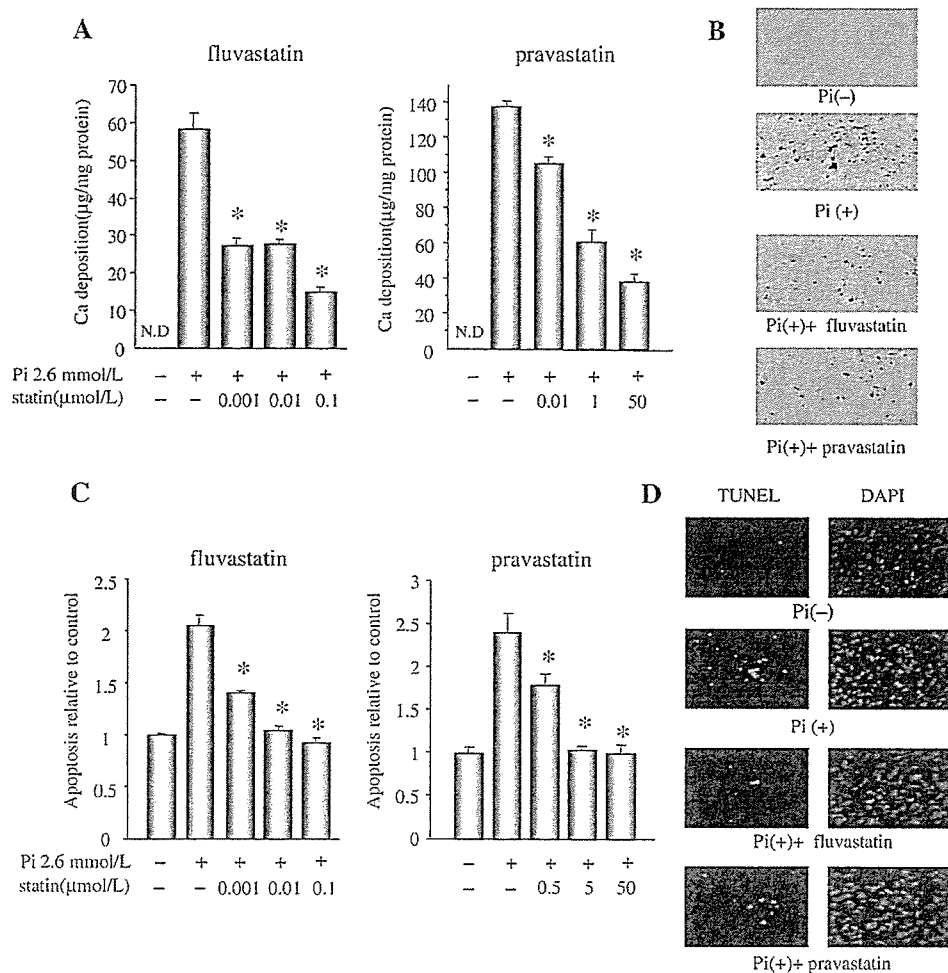

Fig. 1. Statins prevent Pi-induced apoptosis and calcification. HASMC were cultured with the indicated concentrations of fluvastatin and pravastatin in the presence of 2.6 mM Pi for 6 days. Ca deposition was measured by o-cresolphthalein complexone method, and normalized by cell protein content. All values are presented as mean± S.E.M. ($n=6$). *$P<0.05$ vs. statin (−) by Fisher's test. N.D. stands for "not detected" (A). On day 6, the inhibitory effect of fluvastatin (0.1 μM) and pravastatin (50 μM) on 2.6 mM Pi [Pi(+)]-induced Ca deposition was evaluated at the light microscopic level with von Kossa's staining (B). Serum-starved HASMC were cultured with the indicated concentrations of fluvastatin and pravastatin for 12 h and then incubated with 2.6 mM Pi for an additional 24 h. A quantitative index of apoptosis, determined by ELISA, is presented as the relative value to that without statins and 2.6 mM Pi. All values are presented as mean±S.E.M. ($n=3$). *$P<0.05$ vs. 2.6 mM Pi, statin (−) by Fisher's test (C). The antiapoptotic effect of fluvastatin (0.1 μM) and pravastatin (50 μM) was evaluated by TUNEL staining (green) on day 6. Nuclei were counterstained with DAPI (4′,6-diamino-2-phenylindole, blue) (D).
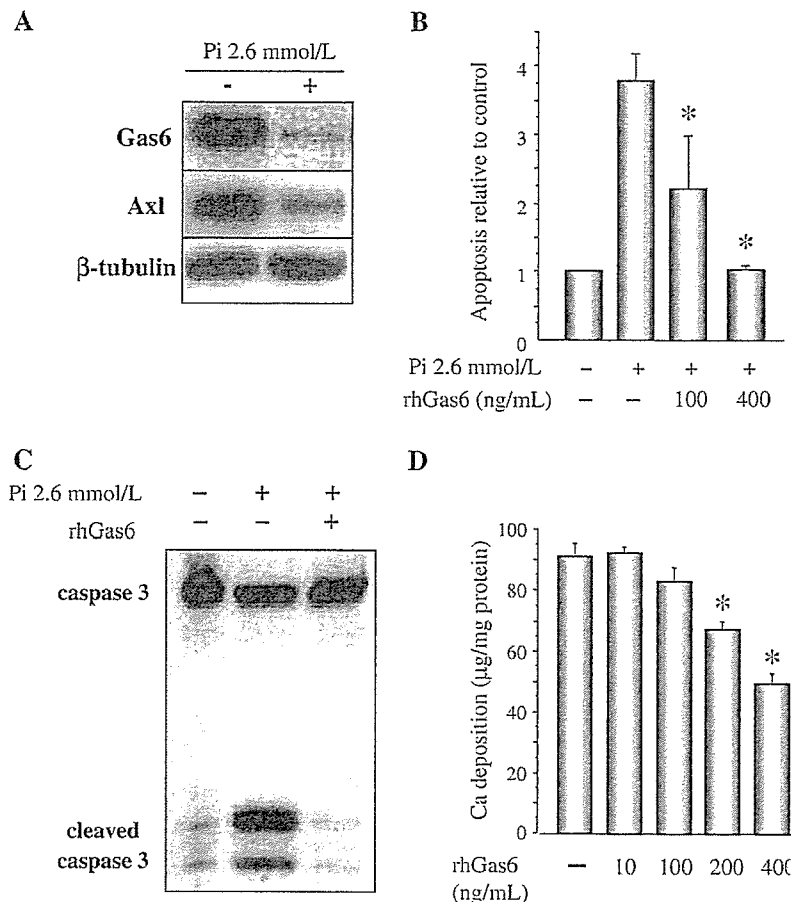
Fig. 2. Pi suppresses Gas6 and Axl expression, and rhGas6 inhibits caspase-dependent apoptosis and calcification. HASMC were cultured in the presence or absence of 2.6 mM Pi for 12 h. Cell lysates were collected and subjected to SDS-PAGE followed by immunoblotting with antibodies to Gas6, Axl or β-tubulin (A). After pretreatment with the indicated concentrations of rhGas6, apoptosis was induced by 2.6 mM Pi. All values are presented as mean±S.E.M. ($n=3$). *$P<0.05$ vs. 2.6 mM Pi, rhGas6 (−) by Fisher's test (B). HASMC were pretreated with rhGas6 (400 ng/ml) for 1 h, then cultured with 2.6 mM Pi for 12 h. Cell lysates were immunoblotted with an antibody that recognizes caspase-3 (35 kDa) and the cleaved forms of caspase-3 (17 and 19 kDa) (C). For measurement of Ca deposition, HASMC were cultured with the indicated concentrations of rhGas6 in the presence of 2.6 mM Pi for 6 days. All values are presented as mean±S.E.M. ($n=6$). *$P<0.05$ by Fisher's test (D). Experiments were performed with at least three different cell populations.

3.3. Downregulation of phospho-Akt participates in Pi-induced apoptosis

Since in NIH-3T3 fibroblasts, the antiapoptotic effect of Gas6-Axl interaction has been shown to be mediated by Akt phosphorylation (Goruppi et al., 1999), we examined whether Akt participates in the signaling of downregulation of the Gas6-Axl interaction during Pi-induced apoptosis. In the presence of 2.6 mM Pi, Akt phosphorylation was downregulated in a time-dependent manner, whereas the expression of total Akt was not changed (Fig. 3A). In addition, rhGas6 abrogated the Pi-induced decrease in Akt phosphorylation, implying that subsequent downregulation of Akt phosphorylation is the pathway of Pi-induced apoptosis (Fig. 3B).

Because Akt phosphorylation is regulated by PI3K, we examined the effect of wortmannin, a specific PI3K inhibitor, on rhGas6-mediated phosphorylation of Akt. As shown in Fig. 3B, wortmannin abrogated the rhGas6-induced phosphorylation of

Akt and further eliminated the inhibitory effect of rhGas6 on Pi-induced apoptosis and calcification (Fig. 3C, D). These results indicate that the preventive effect of rhGas6 on Pi-induced apoptosis and calcification was mediated by the PI3K-Akt pathway.

3.4. Pi suppresses Bcl2 phosphorylation and activates Bad

To establish the downstream components of Pi-induced apoptosis, two key apoptosis-regulating proteins, Bcl2 and Bad, were analyzed. During apoptosis, phosphorylation of Bcl2 (active form) and Bad (inactive form) was markedly reduced by 2.6 mM Pi in a time-dependent manner. The expression level of their total protein was not changed in this period (Fig. 4A, B). By supplementation of the medium with rhGas6, the decrease in phosphorylation of Bcl2 and Bad by Pi was reversed to almost the basal level (Fig. 4C, D). These results indicate that Pi promotes apoptosis by inactivating Bcl2 and activating Bad via a Gas6-dependent pathway.
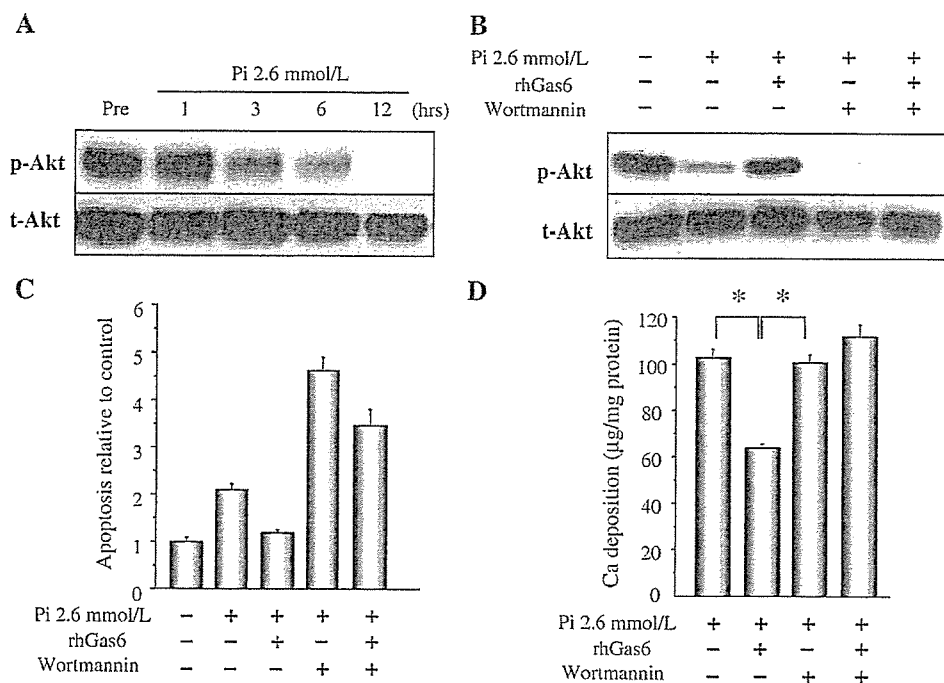
Fig. 3. Pi decreases Akt phosphorylation, and wortmannin abrogates the inhibitory effect of rhGas6 on Akt phosphorylation, apoptosis and calcification. HASMC were cultured in the presence of 2.6 mM Pi for the indicated periods. Cell lysates were immunoblotted with anti-phospho-Akt (p-Akt) antibody and total Akt (t-Akt) antibody (A). HASMC were pretreated with rhGas6 (400 ng/ml), wortmannin (1 μM), or both for 1 h, and then treated with 2.6 mM Pi for 12 h. Cell lysates were immunoblotted with p-Akt and t-Akt antibody (B). After pretreatment with rhGas6 (400 ng/ml) and wortmannin (1 μM), apoptosis was induced by 2.6 mM Pi. All values are presented as mean±S.E.M. ($n=3$). $*P<0.05$ vs. 2.6 mM Pi, rhGas6 (−), wortmannin (−) by Fisher's test (C). HASMC were cultured with rhGas6 (400 ng/ml) and with or without wortmannin (1 μM) in the presence of 2.6 mM Pi for 6 days. Ca content was measured and normalized by cell protein content. All values are presented as mean±S.E.M. ($n=6$). $*P<0.05$ by Fisher's test (D).

3.5. Gas6-mediated survival pathway is the target of statins' effect on apoptosis

To investigate whether the antiapoptotic effect of statins is associated with the Gas6-mediated survival pathway, first, we examined the effect of statins on the expression of Gas6 and Axl. As shown in Fig. 5A and B, both fluvastatin and pravas-

tatin restored the expression of Gas6 and Axl, which was downregulated by 2.6 mM Pi. Because we have shown that the Gas6-mediated survival pathway is Akt-dependent, the effect of statins on Akt phosphorylation was examined. The Pi-induced decrease in Akt phosphorylation was restored by both statins, while total Akt expression was not changed. In addition, we found that both statins stimulated phosphorylation of Bcl2 and
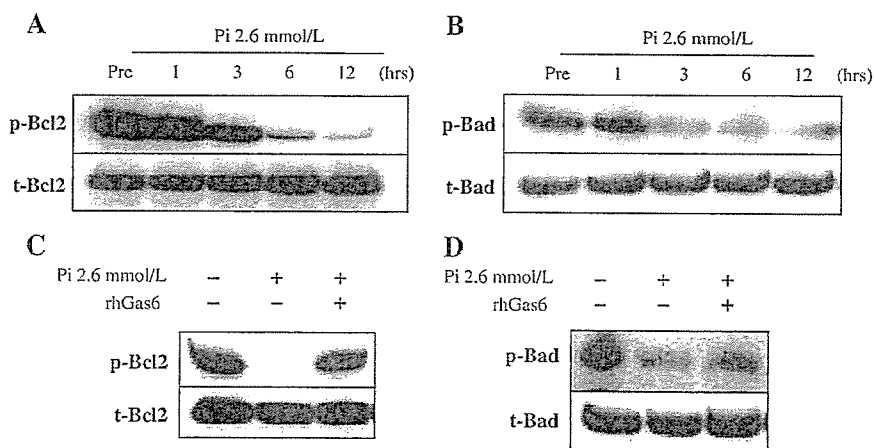

Fig. 4. RhGas6 restores Pi-induced decrease in phosphorylation of Bcl2 and Bad. HASMC were exposed to 2.6 mM Pi for the indicated periods, and cell lysates were subjected to immunoblotting with anti-phospho-Bcl2 (p-Bcl2) antibody and total Bcl2 (t-Bcl2) antibody (A), or with anti-phospho-Bad (p-Bad) antibody and total Bad (t-Bad) antibody (B). HASMC were pretreated with rhGas6 (400 ng/ml) for 1 h, and then treated with 2.6 mM Pi for 12 h. Cell lysates were subjected to immunoblotting with p-Bcl2 and t-Bcl2 antibody (C), or with p-Bad and t-Bad antibody (D).
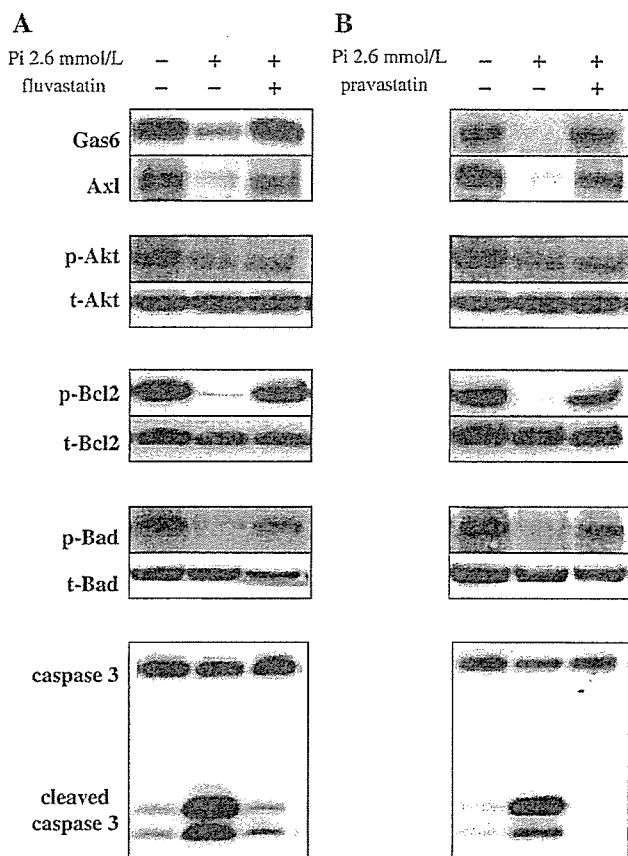
A

| Pi 2.6 mmol/L | − | + | + |
| fluvastatin | − | − | + |

Gas6

Axl

p-Akt

t-Akt

p-Bcl2

t-Bcl2

p-Bad

t-Bad

caspase 3

cleaved
caspase 3

B

| Pi 2.6 mmol/L | − | + | + |
| pravastatin | − | − | + |

Fig. 5. Antiapoptotic effect of statins is associated with upregulation of Gas6-Axl survival pathway. After pretreatment with 0.1 μM fluvastatin (A) and 50 μM pravastatin (B) for 12 h, apoptosis was induced by 2.6 mM Pi. After 12 h, cell lysates were collected and subjected to SDS-PAGE followed by immunoblotting with antibodies that recognize Gas6 and Axl, with phospho-specific Akt (p-Akt) and total Akt (t-Akt) antibody, with phospho-specific Bcl2 (p-Bcl2) and total Bcl2 (t-Bcl2) antibody, or with phospho-specific Bad (p-Bad) and total Bad (t-Bad) antibody. Cell lysates were immunoblotted with an antibody that recognizes uncleaved caspase-3 (35 kDa) and the cleaved forms of caspase-3 (17 and 19 kDa).

Bad, with total expression unchanged. Pi-induced caspase 3 activation was also prevented by both statins. Taken together, these findings suggest that the inhibitory effect of statins on Pi-induced apoptosis is mediated by restoration of the Gas6-mediated survival pathway; PI3K-induced Akt phosphorylation, Bcl2 activation, Bad inactivation, and caspase 3 inactivation.

4. Discussion

In the present study, we found that both lipophilic fluvastatin and hydrophilic pravastatin protected against Pi-induced apoptosis and calcification in HASMC, as we found with atorvastatin previously. With regard to the different potency of statins, we found that the inhibitory effect of pravastatin was inferior to those of fluvastatin and atorvastatin, which exerted similar effects on calcification and apoptosis. This might relate to our previous finding that the inhibition of calcification by statins

was not dependent on the mevalonate pathway (Son et al., 2006). Consequently, the inhibitory effect on calcification was not parallel to the cholesterol-lowering effect. We speculate that the difference between statins was derived from their affinity to vascular smooth muscle cells (VSMC), that is, lipophilic statins have stronger effects on VSMC calcification than hydrophilic statins.

The antiapoptotic effect of statins was induced by restoration of the Gas6-mediated survival pathway: PI3K-induced Akt phosphorylation, Bcl2 and Bad phosphorylation, and caspase 3 inactivation. Gas6 plays a crucial role in the effect of statins on Pi-induced apoptosis. Gas6, a secreted vitamin K-dependent protein, binds to the receptors of the mammalian Axl protein-tyrosine kinase family; Axl, Sky, and Mer, with different affinities (Nagata et al., 1996). Gas6 and Axl have been shown to localize in the neointima of the artery after balloon injury, in which they presumably modulate several cell functions such as differentiation, adhesion, migration, proliferation, and survival in a cell-specific manner (Melaragno et al., 1998). The Gas6-Axl interaction is also shown to upregulate scavenger receptor A expression in VSMC (Ming et al., 2001), and facilitates the clearance of apoptotic cells by macrophages (Ishimoto et al., 2000). Of the above functions, protection against apoptotic cell death has been most studied (Goruppi et al., 1996; Healy et al., 2001; Lee et al., 2002; Nakano et al., 1996). Consistently, the expression of Gas6 and Axl was downregulated by Pi, leading to apoptosis and subsequent calcification.

Several intracellular signaling pathways mediated by Gas6-Axl interaction have been shown previously (Goruppi et al., 1999; Lee et al., 2002; Ming et al., 2001). Akt, which is necessary for Gas6-dependent survival, is a critical downstream effector of the PI3K-dependent antiapoptotic pathway. In VSMC, it has been reported that the PI3K-Akt pathway mediates Gas6 induction of scavenger receptor A (Ming et al., 2001). Consistent with these reports, our study provides evidence that the PI3K-Akt pathway is a target of Gas6-Axl interaction, and downregulation of Akt phosphorylation is associated with Pi-induced apoptosis and calcification. Moreover, it is known that PI3K-Akt affects the cell death program through the Bcl2 family of proteins. This protein family is a critical regulator of apoptosis in a variety of cell types, and the balance of antiapoptotic members, such as Bcl2, versus proapoptotic mediators, such as Bad, determines cell fate (Reed, 1997). Bcl2, whose phosphorylation is required for its antiapoptotic activity (Ruvolo et al., 2001), inhibits programmed cell death by several mechanisms: It binds to caspase CED-4 (Apaf-1) and prevents the cell execution cascade; Bcl2 alters mitochondrial membrane potential and inhibits the release of cytochrome c. On the other hand, Bad plays a proapoptotic role in its dephosphorylated form by binding to Bcl2 and reversing its antiapoptotic effect; phosphorylation of Bad results in its cytosolic sequestration by 14-3-3 and hampers its binding to Bcl2 (Zha et al., 1996). It was also reported that Bad is directly phosphorylated by PI3K-Akt (del Peso et al., 1997). In the present study, Bcl2 was inactivated and Bad was activated (both proteins were dephosphorylated) by Pi, directing the cells to apoptosis, and rhGas6 restored phosphorylation of Bcl2 and Bad. During apoptosis, one of the final biochemical events leading to programmed